RESEARCH ARTICLE | NOVEMBER 01 2024

Percolative dielectric behavior of titanium carbide MXene/cellulose nanofibrils composite films

Vida Jurečič ; Subramanian Lakshmanan ; Nikola Novak ; Vanja Kokol ; Vid Bobnar

APL Mater. 12, 111102 (2024)
https://doi.org/10.1063/5.0232250

Percolative dielectric behavior of titanium carbide MXene/cellulose nanofibrils composite films

Cite as: APL Mater. 12, 111102 (2024); doi: 10.1063/5.0232250
Submitted: 6 August 2024 • Accepted: 15 October 2024 •
Published Online: 1 November 2024

Vida Jurečič,[1,2] Subramanian Lakshmanan,[3] Nikola Novak,[1] Vanja Kokol,[3] and Vid Bobnar[1,2,a)]

AFFILIATIONS

[1] Department of Condensed Matter Physics, Jožef Stefan Institute, Jamova 39, SI-1000 Ljubljana, Slovenia
[2] Jožef Stefan International Postgraduate School, Jamova 39, SI-1000 Ljubljana, Slovenia
[3] Faculty of Mechanical Engineering, University of Maribor, Smetanova 17, SI-2000 Maribor, Slovenia

[a)] **Author to whom correspondence should be addressed:** vid.bobnar@ijs.si

ABSTRACT

Cellulose-based nanomaterials are fascinating renewable biosystems, yet low thermal conductivity and dielectric permittivity often limit their potential applications in flexible electronics. We report dielectric properties of composite films prepared by vacuum filtration or solvent casting method from the native (CNF) or carboxylated (TCNF) cellulose nanofibrils and high electrically and thermally conductive 2D titanium carbide ($Ti_3C_2T_x$) MXenes. Measurements over broad frequency and temperature ranges revealed the influence of preparation method and type of nanofibrils matrix on the overall dielectric response, as well as a notable impact of absorbed water, particularly on the cellulose's secondary β and γ relaxations. A detailed investigation of material with the lowest amount of impurities, vacuum-filtered MXene/CNF composites, confirmed that the dielectric response follows the predictions of the percolation theory. The resulting strong enhancement of the dielectric permittivity on increasing MXene content demonstrates the potential of developed composites for applications in eco-friendly dielectric and piezoelectric devices.

I. INTRODUCTION

The theory of percolation in general explains a physical process in which a macroscopic magnitude is strongly modified as a result of small microscopic changes in connectivity.[1] One such process is the anomalous behavior of a metal–insulator composite (a so-called percolative composite) near its percolation threshold, which is characterized by an abrupt discontinuity in the real part of the electrical conductivity.[2–4] Theory furthermore predicts that the dielectric permittivity ε' of a composite comprising a conductive filler embedded in a dielectric matrix diverges at the percolation threshold, where the insulator–metal transition occurs.[2] The fact that the effective dielectric permittivity of the mixture is much larger than the values of the individual constituents can intuitively be understood by a simple geometrical approach: Close to the percolation point, there are many conducting particles isolated by thin dielectric layers.

The development of high-ε' materials has become one of the major scientific and technological issues, as the requirement for compact and low-cost systems designed to control and store electrical charges has increased substantially. Such materials are highly desirable for use not only as capacitor dielectrics but also in a broad range of electromechanical applications, such as actuators, sonars, and high-frequency transducers. The input electric energy that can be converted into the strain energy is, namely, directly proportional to the dielectric permittivity of the electroactive material $U_e \propto \varepsilon' E^2$. Thus, by increasing the dielectric permittivity, the desired strain can be induced under a much reduced electric field E.

The composite approach, in which conductive particles are dispersed within an insulating dielectric or ferroelectric matrix, has successfully been realized in both polymeric and inorganic systems. In percolative polymer composites, where conductive polyaniline particles were dispersed in polyvinylidene fluoride-based polymers,[5] the dielectric permittivity increases for several orders of magnitude on approaching the percolation threshold. An identical behavior was observed in inorganic percolative composites made of conductive nickel particles and ferroelectric ceramic matrix[6] as well as in all-

ceramic percolative composites, which are composed of conducting and insulating grains.[7,8] Moreover, in nanocomposite films where ammonia-functionalized[9] or reduced graphene oxide[10] was incorporated into the cellulose nanofibrils matrices, ε' substantially increases already at a low filler content due to a large Maxwell–Wagner interfacial polarization.

Biopolymers such as cellulose have been proposed as an auspicious base material for flexible electronics due to their low cost and biodegradability.[11] Cellulose nanofibrils have a high aspect ratio[12] with a high elastic modulus (138 GPa)[13] and a low thermal expansivity (0.1 ppm/K),[14] compared to other polymers. The TEMPO-oxidation of cellulose results in high densities of carboxylate groups on the surfaces of cellulose nanofibrils that allow homogeneous dispersion in composites and further improved physical properties.[15–17] Since the high dielectric permittivity is crucial for energy storage applications, the main strategy in the fabrication of flexible cellulose materials with improved dielectric performance is focused on using nano-additives, such as carbon nanotubes and graphene-based nanosheets, due to their ultra-high specific surface area and excellent electric properties.[11] With the two-dimensional sheet-like structure with covalently attached carbon atoms having various functional groups on the edges and basal planes, the graphene oxide shows excellent dispersibility in polymeric matrices;[18] however, for the fabrication of electronic devices, the low electrical conductivity limits its applicability—hence the ammonia-functionalized[9] or reduced graphene oxide[10] was used for the fabrication of high-ε' flexible cellulose-based films.

In this work, we present the dielectric response of cellulose nanofibrils/$Ti_3C_2T_x$ composite films. Titanium carbide $Ti_3C_2T_x$ belongs to a class of novel 2D transition metal carbides, nitrides, and carbon nitrides, so-called MXenes. These systems (denoted as $M_{n+1}X_nT_x$, where M is an early transition metal; X is C and/or N; T is a hydroxyl, oxygen, or fluorine surface termination unit; and n = 1–3) have attracted much attention due to their outstanding electrochemical properties, hydrophilicity, and metallic conductivity,[19] and are similar to 2D perovskite oxides,[20,21] which are very interesting for two-dimensional electronics. Not only that the lack of a large-scale and cost-effective method for synthesis still limits the use of graphene-based systems in high-performance electronics, MXenes (particularly $Ti_3C_2T_x$) demonstrate even higher electrical conductivity than the solution-processed graphene.[22,23] We report the influence of the preparation method and type of nanofibrils matrix, as well as a notable impact of absorbed water on the overall dielectric response. We demonstrate that the dielectric response of composites follows the predictions of the percolation theory, which results in the strong enhancement of the dielectric permittivity with increasing MXene content.

II. MATERIALS AND METHODS

A. Preparation of cellulose-MXene composite films

Multi-layered (ML) and few-layered (FL) 2D $Ti_3C_2T_x$ MXene powders with 10–20 μm (ML) or ≈1 μm (FL) thick accordion-like morphology of well packed and aligned 10–20 nm thin nanosheets were purchased from Nanochemazone (Canada) and used as received. In addition, titanium aluminum carbide (Ti_3AlC_2) powder (MAX phase) of 10–30 μm in diameter was obtained to self-prepare the MXene by hydrofluoric acid etching method at room temperature.[24] Here, 0.5 g of Ti_3AlC_2 powder was dispersed in 10 ml of 30% hydrofluoric acid by magnetic stirring at 20 rpm for 24 h. The sample was then washed several times with deionized water via centrifugation until the supernatant pH value reached ≈6. The $Ti_3C_2T_x$ sediments were rewashed with deionized water via vacuum-assisted filtration using a polyvinyl difluoride filter membrane with 0.22 μm pore size before collection of the remaining MXene. Then the sample was intercalated/delaminated by magnetic stirring at 20 rpm for 24 h in dimethylsulfoxide, followed by 1 h sonication at 20% amplitude using the sonicator Vibra Cell VCX 750 (Sonics, USA). Finally, the obtained MXene powder was vacuum dried at 375 K for 24 h. Figure 1 shows cross-sectional SEM images of purchased ML titanium carbide MXene powder and self-prepared MXenes. SEM imaging was performed using a low-vacuum scanning electron microscope, FEI Quanta 200 3D (Thermo Fisher Scientific Inc., USA), equipped with an EDX spectrometer (Inca 350, Oxford Instruments Nanoanalysis, UK) for micro-chemical mapping. Both images demonstrate accordion-like morphology of well packed and aligned 10–20 nm thin MXene nano-sheets.

Cellulose nanofibrils (CNF) or TEMPO [(2,2,6,6-Tetramethylpiperidin-1-yl)oxyl] oxidized CNF (TCNF) with lengths of 1–3 μm and diameters of 10–70 nm were derived from bleached softwood pulp at the University of Maine, USA. Pristine cellulose and CNF,TCNF/MXene composite films were prepared either by solvent casting (SC) or vacuum filtration (VF) methods. Various quantities of the $Ti_3C_2T_x$ powder were dispersed homogeneously in 15 ml of dimethyl sulfoxide by an

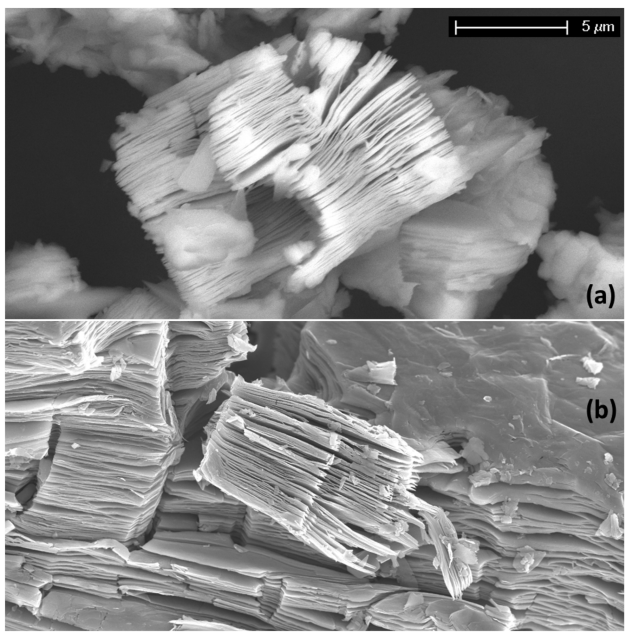

FIG. 1. Cross-sectional SEM images of (a) multi-layered titanium carbide MXene powder purchased from Nanochemazone and (b) self-prepared MXenes. The scale bar is the same for both images.

ultrasonic processor, then mixed with an appropriate amount of Milli-Q water-suspended CNF/TCNF and stirred for 1 h to get homogeneous cellulose/MXene dispersions. The dispersions were poured directly into the polystyrene Petri dishes and dried at room temperature (SC films) or vacuum filtered through a cellulose filter with a pore size of 5–8 μm, transferred in a wet stage to Petri dishes of 6 cm in diameter, left to dry at room temperature, and finally pressed at 4 bar for 5 h with a hydraulic press. The thicknesses of developed films were ≈40 μm in the case of pristine cellulose, while they increased to almost 300 μm in samples with 90 wt. % of MXene.

Figure 2 shows cross-sectional SEM images of vacuum-filtered pristine cellulose nanofibrils film and MXene/CNF composite film with 10 wt. % of $Ti_3C_2T_x$. The morphology of the $Ti_3C_2T_x$ MXene/cellulose nanofibrils composite films significantly differs from that of an ideal percolative composite with randomly distributed small-scale metallic regions within a dielectric matrix (see, for example, Fig. 1 in Refs. 7 and 8). Here, high electrical conductivity filler is in the form of relatively large 2D sheets and, furthermore, forms electrostatic interactions with the matrix as well as hydrogen bonds with hydroxyl and carboxyl surface groups on CNF/TCNF.

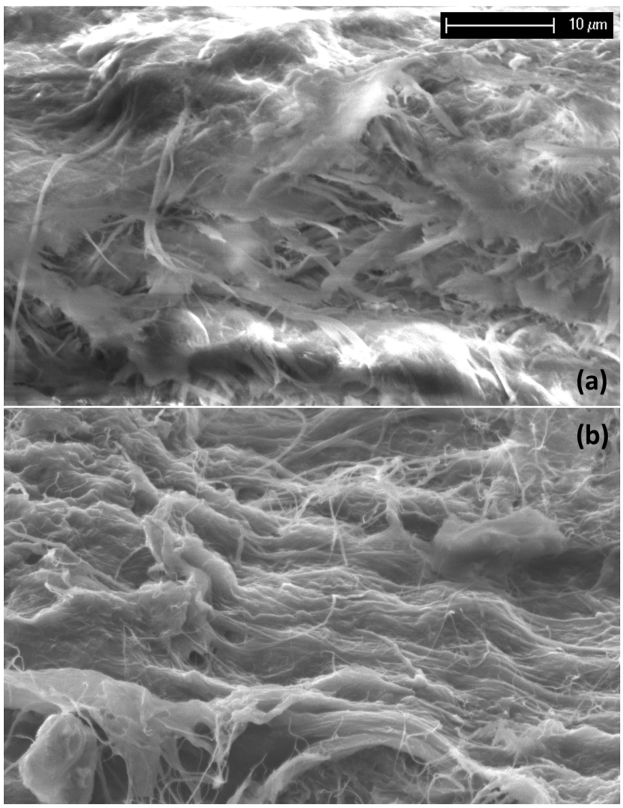

FIG. 2. Cross-sectional SEM images of vacuum-filtered (a) pristine cellulose nanofibrils film and (b) MXene/CNF composite film with 10 wt. % of $Ti_3C_2T_x$. The scale bar is the same for both images.

B. Dielectric characterization

For dielectric measurements, the surfaces of films were covered by ≈100 nm thick sputtered gold electrodes having a diameter of 4 mm. The complex linear dielectric constant $\varepsilon^*(\omega, T) = \varepsilon' - i\varepsilon''$ was measured by a Novocontrol Alpha Analyzer. The amplitude of the probing ac electric signal was 1 V. The values of the real part of the dielectric constant, i.e., the dielectric permittivity ε', and the values of the real part of the electrical conductivity, σ', were calculated from the actual measured quantities, capacitance C and electrical resistivity R via $\varepsilon' = Cd/(\varepsilon_0 S)$ and $\sigma' = d/(RS)$, where d is the sample thickness, S is the electrode area, and $\varepsilon_0 = 8.85 \times 10^{-12}$ As/(Vm) is the permittivity of free space. The imaginary part of the dielectric constant ε'' is connected to the electrical conductivity via $\sigma' = 2\pi\nu\varepsilon_0\varepsilon''$.

The dielectric response was detected either as a function of frequency at a constant temperature or at several frequencies during heating or cooling runs with a rate of ±0.75 K/min. The temperature of samples was stabilized within ±0.01 K by using the lock-in bridge technique with a platinum resistor Pt100 as a thermometer.

III. RESULTS AND DISCUSSION

A. General dielectric response

Figure 3 shows the frequency dependence of the dielectric permittivity and electrical conductivity, detected at room temperature in a pristine CNF film. The absorbed water strongly enhances values of both, ε' and σ', at low frequencies in the as-prepared sample (note the logarithmic ε'-scale). While free absorbed water requires low energy to be removed, water molecules can also be trapped in the fiber network[25] or bound to the hydroxyl groups on the surface of cellulose. Trapped and bound water can be removed under specific drying conditions to overcome capillary forces and other interactions. After drying the sample, ε' and σ' values at low frequencies decrease by orders of magnitude but increase again when the sample is exposed to air moisture. A similar behavior was detected in the composite sample with 5 wt. % of $Ti_3C_2T_x$ MXene (denoted as CNF-5MX, the inset to Fig. 3; both samples were prepared by vacuum filtration). It can be seen that low-frequency ε' values of as-prepared samples are significantly lower in the composite. MXene sheets not only reduce the space for trapped water within the fibril network but also lower the amount of bounded water due to the $Ti_3C_2T_x$–CNF interactions. To minimize the influence of air moisture on dielectric results prior to all further presented dielectric measurements, the films were dried for 1 h at 375 K.

To compare the influence of $Ti_3C_2T_x$ MXene on the dielectric properties of different cellulose films, first, the dielectric response of composite samples prepared with 5 wt. % of $Ti_3C_2T_x$ was investigated. Figure 4 thus shows the temperature dependence of the dielectric permittivity and electrical conductivity of vacuum-filtered CNF-based, solvent-casted CNF-based, and solvent-casted TCNF-based composite films (a high water retention ability of TCNF prevents it from being vacuum filtered). While the intrinsic data at the highest frequencies are almost identical, we can see that the increase in both, ε' and σ', at low frequencies and high temperatures is much more pronounced in the solvent-casted sample than in the vacuum-filtered CNF-5MX sample. This suggests that solvent-casted samples

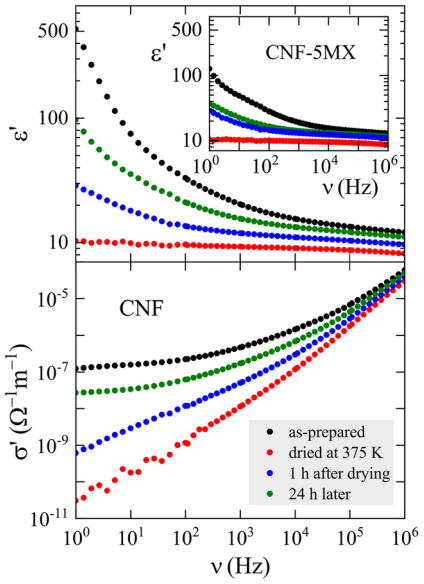

FIG. 3. Frequency dependences of the dielectric permittivity and electrical conductivity, detected at room temperature in (i) as-prepared CNF film, (ii) after drying at 375 K, (iii) 1 h after drying, and (iv) 24 h later. The inset shows ε' data, detected in the CNF-5MX composite in an identical series of steps.

contain a higher amount of free space charges or other impurities than vacuum-filtered ones. Since these charges increase dielectric losses and imply the dielectric breakdown at lower electric fields, we have further thoroughly analyzed the dielectric response of vacuum filtered $Ti_3C_2T_x$/CNF composite films. The number of space charges is the highest in the TCNF-based sample—this is not surprising since a high number of hydroxyl groups on the surface of CNF are replaced by highly hydrophilic and polar carboxylate groups after TEMPO-mediated oxidation of cellulose.[15,17]

The dielectric spectra in Fig. 4 also reveal a relaxation behavior between 150 and 300 K, particularly in both CNF-based composites. It is known that amorphous cellulose exhibits two secondary relaxations, so-called γ and β relaxations, at temperatures below its glass transition temperature. The activation energy of γ relaxation and the comparison with other polysaccharides lead to the conclusion that it corresponds to the noncooperative rotation of CH_2OH lateral groups.[26] On the other hand, β relaxation is characterized by high values of the activation parameters, suggesting that this dissipation process originates from cooperative but localized motions of segments of the main chain.[27] The dielectric relaxation strength of the γ relaxation is typically much higher than that of the β relaxation; however, it is difficult to distinguish the heavily overlapped relaxation signals since they both occur in the temperature range of 150–300 K.

To investigate the impact of moisture and MXenes on the cellulose relaxation behavior, we have performed the temperature dependent measurements, which are presented in Fig. 5. The mainframe shows the dielectric response of the as-prepared (undried) CNF-10MX composite, detected at several frequencies during a cooling run from room temperature to 125 K, subsequent heating run to 375 K, and final cooling run to 125 K. It can be seen that the relaxation intensity is much lower during the second cooling run after the sample has been heated to a high temperature, i.e., dried. This suggests that similar to many other polymer systems,[28–30] these molecular motions (particularly those of γ relaxation) involve water molecules that are absorbed into the free volume of the system and attached to cellulose polar groups via weak physical or stronger hydrogen bonds. The inset to Fig. 5 compares the response of the

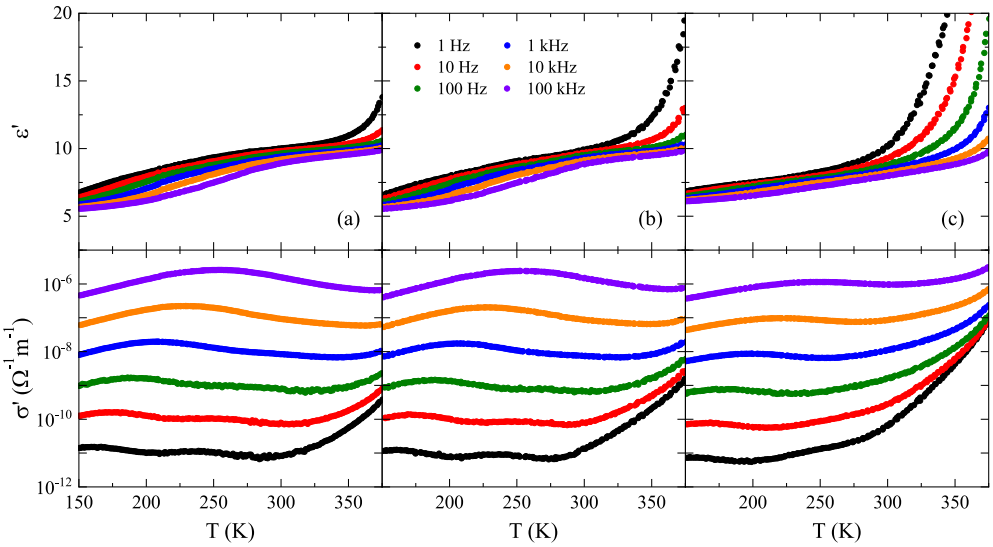

FIG. 4. Dielectric response detected during cooling runs after various composite samples with 5 wt. % of MXene were heated to 375 K: (a) vacuum-filtered CNF-5MX, (b) solvent-casted CNF-5MX, and (c) solvent-casted TCNF-5MX.

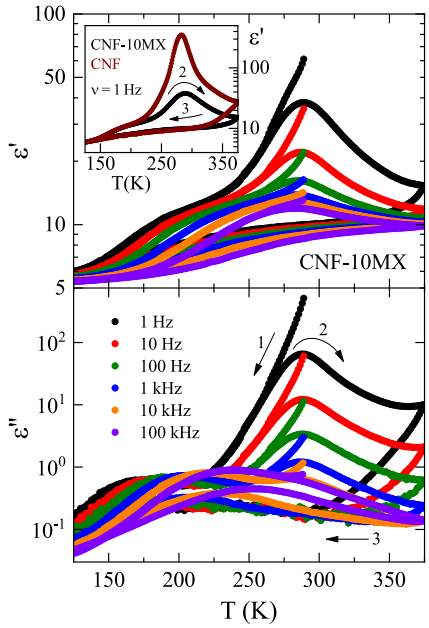

FIG. 5. Dielectric response of the vacuum-filtered CNF-10MX composite, detected at several frequencies during (1) cooling run from room temperature to 125 K, (2) subsequent heating run to 375 K, and (3) final cooling run to 125 K (indicated by arrows). The inset shows a comparison of the dielectric permittivity of this composite with the pristine VF CNF sample at the lowest measurement frequency of 1 Hz during the second (125–375 K) and third (375–125 K) temperature runs.

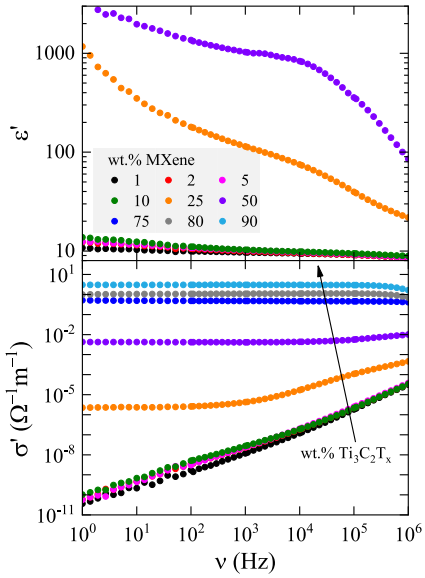

FIG. 6. Frequency dependences of the dielectric permittivity and electrical conductivity, detected at room temperature in the vacuum-filtered $Ti_3C_2T_x$/CNF composite films with various MXene content.

CNF-10MX composite with the pristine CNF sample at the lowest measurement frequency of 1 Hz during the second and third temperature runs. It can be seen that 10 wt. % of $Ti_3C_2T_x$ negligibly influences the cellulose relaxation behavior, yet, as already revealed in Fig. 3, the influence of moisture is much more pronounced in the pristine CNF.

B. Percolative behavior

The frequency dependence of the room-temperature dielectric response in the $Ti_3C_2T_x$/CNF composite films with various MXene content is shown in Fig. 6. While at higher frequencies the electrical conductivity increases, at lower frequencies values tend toward the dc-conductivity plateau. Such a behavior corresponds to an equivalent circuit composed of two R–C circuits connected in serial. The resistivity of the low-frequency plateau is then $R_1 + R_2$ (R_1 and R_2 are resistivities of titanium carbide and CNF, respectively), while at higher frequencies the conductivity follows a ν^2 law if $R_2 \gg R_1$,[2] as is evidently the case in a percolative composite (then the value of the low-frequency plateau is just the resistivity of the CNF matrix). Concomitantly, the frequency dependence of the effective capacity of such an equivalent circuit would obey a Debye-like behavior from C_1 at low to C_2 at high frequencies if $C_1 \gg C_2$. Aside from modeling the spectra by an equivalent circuit with frequency-independent elements, the detected dielectric response can also be qualitatively physically understood. While at lower frequencies the conductivity of the $Ti_3C_2T_x$ inclusions is effectively blocked, at sufficiently high frequencies their higher conductivity is revealed since most of the charge carriers have no time to feel the blocking boundaries. The effective ac-conductivity σ', therefore, increases with frequency (and would increase up to the high-frequency plateau corresponding to the value of the MXene's conductivity). As even for an inhomogeneous system the Kramers–Kronig relations must be satisfied, the increasing σ' parts of spectra contribute to the static dielectric permittivity via a strong dielectric relaxation. It should be stressed out that composite films with 75, 80, and 90 wt. % of $Ti_3C_2T_x$ are evidently above the percolation threshold; therefore, their high electrical conductivity prevents the determination of the dielectric permittivity. Finally, the measured sample forms an electrical circuit with the resistance and, eventually, the inductance of the measuring setup, resulting in a resonant-like behavior of the detected response. Such behavior usually occurs at frequencies far beyond the measurement range (≈10 GHz); however, in samples close to the percolation threshold, the capacitance is so high that it can already influence the data at the highest measuring frequencies.

The theory of percolation was initially developed to describe several abrupt transitions commonly found in transport phenomena. Based on this model, a general theory was built that explains a physical process in which a macroscopic magnitude is strongly modified as a result of small microscopic changes in connectivity.[1] One such process is the anomalous behavior of a metal–insulator composite near its percolation threshold, which is characterized by an abrupt discontinuity in the real part of the electrical conductivity.[3,4] An excellent review of the system consisting of randomly distributed metallic and dielectric regions is given in the paper of Efros and Shklovskii:[2] It is shown that the static dielectric constant diverges at the percolation threshold—at the volume fraction of metallic regions

(p) where the insulator-to-metal transition occurs, i.e., the static effective electrical conductivity σ undergoes a transition from

$$\sigma = \sigma_{diel}\left(\frac{p_c - p}{p_c}\right)^{-q}, \quad (1)$$

which is valid below the percolation threshold p_c into

$$\sigma = \sigma_{metal}\left(\frac{p - p_c}{p_c}\right)^{t}, \quad (2)$$

which holds true for $p > p_c$. σ_{diel} and σ_{metal} are the conductivities of the dielectric and metallic phases, respectively.

$Ti_3C_2T_x$ MXene/cellulose nanofibrils composite films do not represent an ideal percolative composite with randomly distributed metallic regions within a dielectric matrix. High electrical conductivity filler $Ti_3C_2T_x$ is in the form of relatively large 2D sheets, which, in addition to electrostatic interactions with the matrix, also form hydrogen bonds with hydroxyl and carboxyl surface groups on CNF/TCNF. Nevertheless, the dielectric permittivity strongly increases with increasing MXene content—Fig. 7 depicts ε' values, detected at the highest measuring frequency of 1 MHz, where the contribution of free space charges or extrinsic effects, such as the presence of surface layers, is the lowest.[31] The inset to Fig. 7 zooms in the ε' data from Fig. 6 for samples with the lowest MXene content (1, 2, 5, and 10 wt. %) in the high-frequency region. Moreover, the electrical conductivity reasonably well follows the theoretical predictions of Eqs. (1) and (2)—this behavior is depicted in the inset to Fig. 8, which also reveals that a smooth transition from Eq. (1) to Eq. (2) occurs in a small interval Δ near the percolation point. The experimental data, shown in the mainframe, were collected at the lowest measurement frequency of 1 Hz since they are closest to the intrinsic dc conductivity of the material. It should be stressed that the percolative behavior slightly depends on the type of MXenes used in the composites. Due to the Maxwell–Wagner interfacial polarization, the dielectric permittivity increases with increasing $Ti_3C_2T_x$ content in all samples; however, the electrical conductivity reasonably follows the theoretical predictions only in samples with smaller MXenes—the morphology of composites with multi-layered

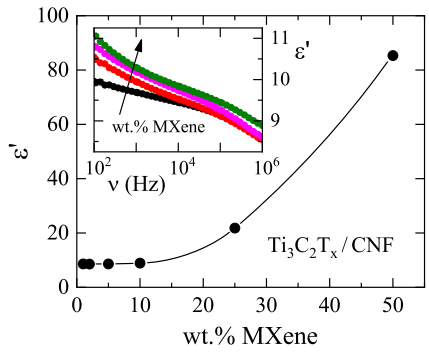

FIG. 7. Room temperature dielectric permittivity of composite films at the highest measurement frequency of 1 MHz as a function of the MXene content. The solid lines are a guide to the eye. The inset zooms in the ε' data from Fig. 6 for samples with the lowest MXene content (1, 2, 5, and 10 wt. %) in the high-frequency range.

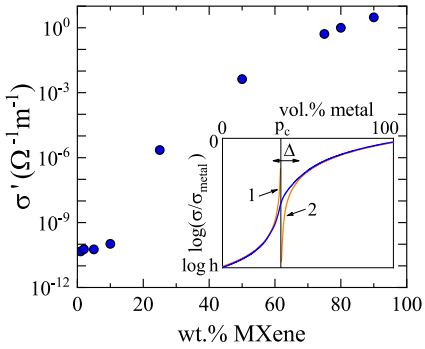

FIG. 8. Electrical conductivity of $Ti_3C_2T_x$/CNF composite films as a function of the MXene content. Data were collected at room temperature at the lowest measurement frequency of 1 Hz (see Fig. 6). The inset shows the theoretical dependence of the effective electrical conductivity (blue line) for a system consisting of randomly distributed metallic and dielectric regions ($h = \sigma_{diel}/\sigma_{metal} \ll 1$). A smooth transition between behaviors described by Eqs. (1) and (2) (orange lines) occur in a small interval Δ near the percolation point p_c.

MXenes appears to be too different from that of an ideal percolative composite.

Table I summarizes the dielectric properties of various cellulose nanofibrils composite films, although such a comparison might not be completely relevant. Not only data are often reported at different frequencies, but due to a strong frequency dispersion in heterogeneous systems (Fig. 6), even data detected at the same frequency do not provide a fair comparison—the most reasonable would be to compare the intrinsic dielectric permittivity (detected at high frequencies) and values of the dc electrical conductivity. Moreover, near the percolation threshold, even a slight change in the amount of filler leads to huge variations of ε' and σ'. For example, σ' values of our samples compared to those of CNF/NGO composites easily mislead us that the CNF/$Ti_3C_2T_x$ system is much more conductive. However, CNF/NGO samples were prepared only with a relatively small amount of conductive filler, while CNF/$Ti_3C_2T_x$ composites were developed up to high MXene weight ratios. Nevertheless, data in Table I reveal that the composite approach successfully increases the dielectric response of pure cellulose nanofibrils. It is, however, important to stress that, in order to be applicable in flexible electronics, the developed composites should retain the flexibility of the pure CNF matrix.

As is typical for all percolative systems,[6–8] a strong conductivity increase close to the percolation point increases dielectric losses. While in samples with up to 10 wt. % of MXene content, tan $\delta = \varepsilon''/\varepsilon'$ is almost constant (≈0.07), it increases to 0.4 and 2.1 in composites with 25 and 50 wt. % of MXene, respectively. Despite this fact, the developed composites still show application potential, particularly in the field of flexible piezoelectric materials. Cellulose nanofibril films, namely, exhibit a promising piezoelectric response.[35] In addition, since the electrical energy $U_e = \frac{1}{2}\varepsilon_0\varepsilon' E^2$ that can be during an electromechanical operation converted into the strain energy is directly proportional to the dielectric permittivity, by increasing of ε' we can increase the piezoelectric response or, eventually, induce the desired strain under much reduced electric field. This principle has already been presented for the case of electroactive relaxor polymers,

TABLE I. Dielectric permittivity and ac electrical conductivity of various cellulose nanofibrils composite films. NGO and RGO denote the ammonia-functionalized and reduced graphene oxide, respectively, while AgNW stands for the silver nanowires. For two systems, only the dielectric loss value was reported.

Composite film	ε'	σ' (Ω^{-1} m^{-1})	Source
Pure CNF	8 (1 MHz)	3×10^{-11} (1 Hz)	this work
CNF/TiO_2	20 (1 kHz)	$\tan\delta \approx 1$ (1 kHz)	Ref. 32
CNF/$BaTiO_3$	50 (1 MHz)	2×10^{-7} (10 Hz)	Ref. 33
CNF/AgNW	700 (1 GHz)	$\tan\delta \approx 0.3$ (1 GHz)	Ref. 34
CNF/NGO	50 (1 MHz)	3×10^{-7} (10 Hz)	Ref. 9
CNF/RGO	160 (1 MHz)	3×10^{-3} (100 Hz)	Ref. 10
CNF/$Ti_3C_2T_x$	85 (1 MHz)	4×10^{-3} (1 Hz)	this work

either in composites of poly(vinylidene fluoride-trifluoroethylene) copolymer with copper-phthalocyanine oligomers[36] or in composites, where conductive polyaniline particles were used as a filler in the poly(vinylidene fluoride-trifluoroethylene-chlorotrifluoroethylene) terpolymer matrix.[5]

IV. SUMMARY

Flexible composite films were prepared by vacuum filtration or solvent casting method from the native or carboxylated cellulose nanofibrils and high electrically and thermally conductive 2D titanium carbide MXenes. Measurements over broad frequency and temperature ranges revealed the influence of the preparation method and type of nanofibrils on the overall dielectric response. While the intrinsic data at the highest frequencies are almost identical, the increase in both, ε' and σ', at low frequencies and high temperatures is much more pronounced in the solvent-casted samples than in the vacuum-filtered samples, which suggests that SC samples contain a higher amount of free space charges or other impurities. Since these charges increase dielectric losses and imply the dielectric breakdown at lower electric fields, we have further thoroughly analyzed the dielectric response of VF $Ti_3C_2T_x$/CNF composite films. The number of space charges in the TCNF-based samples is higher since the many hydroxyl groups on the surface of CNF are replaced by highly hydrophilic and polar carboxylate groups after TEMPO-mediated oxidation of cellulose.

The absorbed water strongly enhances values of the dielectric permittivity and electrical conductivity at low frequencies in the as-prepared samples. After drying the cellulose sample, ε' and σ' values at low frequencies decrease by orders of magnitude; however, they increase again when the sample is exposed to air moisture. The effect is less pronounced in composite samples since the MXene sheets not only reduce the space for trapped water within the fibril network but also lower the amount of bounded water due to the $Ti_3C_2T_x$–CNF interactions. Moreover, water molecules that are absorbed into the free volume of the system and attached to cellulose polar groups via weak physical or stronger hydrogen bonds are involved in the molecular motions of two secondary dielectric relaxations, particularly in the noncooperative rotation of lateral groups that correspond to γ relaxation.

Since the high electrical conductivity filler is in the form of relatively large 2D sheets, which besides electrostatic interactions also form hydrogen bonds with cellulose's surface groups, investigated systems do not represent an ideal percolative composite. Nevertheless, the dielectric response of vacuum-filtered $Ti_3C_2T_x$/CNF films resembles the response of a composite with randomly distributed metallic regions within a dielectric matrix. The effective ac electrical conductivity increases with frequency, from the low-frequency plateau, corresponding to the electrical conductivity of the matrix, toward the high-frequency plateau, corresponding to the value of the MXene's conductivity. The dependence of σ' on the MXene content reasonably well follows the predictions of the percolation theory [Eqs. (1) and (2)]. Concomitantly, the dielectric permittivity strongly increases with increasing MXene content, which demonstrates the potential of developed composites for applications in eco-friendly dielectric and piezoelectric devices.

ACKNOWLEDGMENTS

This work was supported by the Slovenian Research and Innovation Agency (Program Nos. P1-0125 and P2-0424 and Project No. J2-3053).

AUTHOR DECLARATIONS

Conflict of Interest

The authors have no conflicts to disclose.

Author Contributions

Vida Jurečič: Data curation (equal); Formal analysis (equal); Investigation (equal); Methodology (equal); Visualization (equal); Writing – original draft (supporting). **Subramanian Lakshmanan**: Data curation (equal); Formal analysis (equal); Investigation (equal); Writing – review & editing (equal). **Nikola Novak**: Formal analysis (equal); Funding acquisition (equal); Investigation (equal); Methodology (equal); Writing – review & editing (equal). **Vanja Kokol**: Conceptualization (equal); Funding acquisition (equal); Investigation (equal); Supervision (equal); Visualization (equal); Writing – review & editing (equal). **Vid Bobnar**: Conceptualization (equal); Funding acquisition (equal); Investigation (equal); Methodology (equal); Supervision (equal); Visualization (equal); Writing – original draft (lead).

DATA AVAILABILITY

The data that support the findings of this study are available from the corresponding author upon reasonable request.

REFERENCES

[1] S. Feng, B. I. Halperin, and P. N. Sen, "Transport properties of continuum systems near the percolation threshold," Phys. Rev. B **35**, 197 (1987).
[2] A. L. Efros and B. I. Shklovskii, "Critical behaviour of conductivity and dielectric constant near the metal-non-metal transition threshold," Physica Status Solidi B **76**, 475 (1976).
[3] S. Kirkpatrick, "Percolation and conduction," Rev. Mod. Phys. **45**, 574 (1973).
[4] D. J. Bergman and Y. Imry, "Critical behavior of the complex dielectric constant near the percolation threshold of a heterogeneous material," Phys. Rev. Lett. **39**, 1222 (1977).

[5]C. Huang, Q. M. Zhang, and J. Su, "High-dielectric-constant all-polymer percolative composites," Appl. Phys. Lett. **82**, 3502 (2003).
[6]C. Pecharromán, F. Esteban-Betegón, J. F. Bartolomé, S. López-Esteban, and J. S. Moya, "New percolative $BaTiO_3$–Ni composites with a high and frequency-independent dielectric constant ($\varepsilon_r \approx 80000$)," Adv. Mater. **13**, 1541 (2001).
[7]V. Bobnar, M. Hrovat, J. Holc, and M. Kosec, "Giant dielectric response in $Pb(Zr,Ti)O_3$–$Pb_2Ru_2O_{6.5}$ all-ceramic percolative composite," Appl. Phys. Lett. **92**, 182911 (2008).
[8]V. Bobnar, M. Hrovat, J. Holc, and M. Kosec, "All-ceramic lead-free percolative composite with a colossal dielectric response," J. Eur. Ceram. Soc. **29**, 725 (2009).
[9]Y. B. Pottathara, V. Bobnar, S. Gorgieva, Y. Grohens, M. Finšgar, S. Thomas, and V. Kokol, "Mechanically strong, flexible and thermally stable graphene oxide/nanocellulosic films with enhanced dielectric properties," RSC Adv. **6**, 49138 (2016).
[10]Y. B. Pottathara, V. Bobnar, M. Finšgar, Y. Grohens, S. Thomas, and V. Kokol, "Cellulose nanofibrils-reduced graphene oxide xerogels and cryogels for dielectric and electrochemical storage applications," Polymer **147**, 260 (2018).
[11]A. Kafy, K. K. Sadasivuni, H.-C. Kim, A. Akther, and J. Kim, "Designing flexible energy and memory storage materials using cellulose modified graphene oxide nanocomposites," Phys. Chem. Chem. Phys. **17**, 5923 (2015).
[12]D. Klemm, F. Kramer, S. Moritz, T. Lindström, M. Ankerfors, D. Gray, and A. Dorris, "Nanocelluloses: A new family of nature-based materials," Angew. Chem., Int. Ed. **50**, 5438 (2011).
[13]T. Nishino, K. Takano, and K. Nakamae, "Elastic modulus of the crystalline regions of cellulose polymorphs," J. Polym. Sci., Part B: Polym. Phys. **33**, 1647 (1995).
[14]T. Nishino, I. Matsuda, and K. Hirao, "All-cellulose composite," Macromolecules **37**, 7683 (2004).
[15]S. Iwamoto, W. Kai, A. Isogai, and T. Iwata, "Elastic modulus of single cellulose microfibrils from tunicate measured by atomic force microscopy," Biomacromolecules **10**, 2571 (2009).
[16]H. Fukuzumi, T. Saito, T. Iwata, Y. Kumamoto, and A. Isogai, "Transparent and high gas barrier films of cellulose nanofibers prepared by TEMPO-mediated oxidation," Biomacromolecules **10**, 162 (2009).
[17]A. Isogai, T. Saito, and H. Fukuzumi, "TEMPO-oxidized cellulose nanofibers," Nanoscale **3**, 71 (2011).
[18]L. Valentini, M. Cardinali, E. Fortunati, and J. M. Kenny, "Nonvolatile memory behavior of nanocrystalline cellulose/graphene oxide composite films," Appl. Phys. Lett. **105**, 153111 (2014).
[19]X. Jiang, A. V. Kuklin, A. Baev, Y. Ge, H. Agren, H. Zhang, and P. N. Prasad, "Two-dimensional MXenes: From morphological to optical, electric, and magnetic properties and applications," Phys. Rep. **848**, 1 (2020).
[20]S. Li, X. Liu, H. Yang, H. Zhu, and X. Fang, "Two-dimensional perovskite oxide as a photoactive high-κ gate dielectric," Nat. Electron. **7**, 216 (2024).
[21]Z. Liu, "Two-dimensional perovskite oxide high-κ dielectric for high-performance phototransistors," Sci. Bull. **69**, 2001 (2024).
[22]A. Shayesteh Zeraati, S. A. Mirkhani, P. Sun, M. Naguib, P. V. Braun, and U. Sundararaj, "Improved synthesis of $Ti_3C_2T_x$ MXenes resulting in exceptional electrical conductivity, high synthesis yield, and enhanced capacitance," Nanoscale **13**, 3572 (2021).
[23]X. Chen, Z. Shi, Y. Tian, P. Lin, D. Wu, X. Li, B. Dong, W. Xu, and X. Fang, "Two-dimensional Ti_3C_2 MXene-based nanostructures for emerging optoelectronic applications," Mater. Horiz. **8**, 2929 (2021).
[24]M. Alhabeb, K. Maleski, B. Anasori, P. Lelyukh, L. Clark, S. Sin, and Y. Gogotsi, "Guidelines for synthesis and processing of two-dimensional titanium carbide ($Ti_3C_2T_x$ MXene)," Chem. Mater. **29**, 7633 (2017).
[25]K. Kulasinski, "Free energy landscape of cellulose as a driving factor in the mobility of adsorbed water," Langmuir **33**, 5362 (2017).
[26]D.-L. Li, S.-C. Shi, K.-Y. Lan, C.-Y. Liu, Y. Li, L. Xu, J. Lei, G.-J. Zhong, H.-D. Huang, and Z.-M. Li, "Enhanced dielectric properties of all-cellulose composite film via modulating hydroxymethyl conformation and hydrogen bonding network," ACS Macro Lett. **12**, 880 (2023).
[27]H. Montès, K. Mazeau, and J. Y. Cavaillé, "The mechanical β relaxation in amorphous cellulose," J. Non-Cryst. Solids **235–237**, 416 (1998).
[28]A. Jonas and R. Legras, "Relation between PEEK semicrystalline morphology and its subglass relaxations and glass transition," Macromolecules **26**, 813 (1993).
[29]J. P. Habas, J. Peyrelasse, and M. F. Grenier-Loustalot, "Rheological study of a high-performance polyimide. Interpretation of the secondary mechanical relaxations of a nadimide crosslinked system," High Perform. Polym. **8**, 515 (1996).
[30]Y. Zhang, S. Ke, H. Huang, L. Zhao, L. Yu, and H. L. W. Chan, "Dielectric relaxation in polyimide nanofoamed films with low dielectric constant," Appl. Phys. Lett. **92**, 052910 (2008).
[31]P. Lunkenheimer, V. Bobnar, A. V. Pronin, A. I. Ritus, A. A. Volkov, and A. Loidl, "Origin of apparent colossal dielectric constants," Phys. Rev. B **66**, 052105 (2002).
[32]J. Tao, S. Cao, W. Liu, and Y. Deng, "Facile preparation of high dielectric flexible films based on titanium dioxide and cellulose nanofibrils," Cellulose **26**, 6087 (2019).
[33]J. Tao, S. Cao, R. Feng, and Y. Deng, "High dielectric thin films based on barium titanate and cellulose nanofibrils," RSC Adv. **10**, 5758 (2020).
[34]T. Inui, H. Koga, M. Nogi, N. Komoda, and K. Suganuma, "High-dielectric paper composite consisting of cellulose nanofiber and silver nanowire," in *14th IEEE International Conference on Nanotechnology* (IEEE, Toronto, ON, Canada, 2014), pp. 470–473.
[35]S. Rajala, T. Siponkoski, E. Sarlin, M. Mettänen, M. Vuoriluoto, A. Pammo, J. Juuti, O. J. Rojas, S. Franssila, and S. Tuukkanen, "Cellulose nanofibril film as a piezoelectric sensor material," ACS Appl. Mater. Interfaces **8**, 15607 (2016).
[36]Q. M. Zhang, H. Li, M. Poh, F. Xia, Z.-Y. Cheng, H. Xu, and C. Huang, "An all-organic composite actuator material with a high dielectric constant," Nature **419**, 284 (2002).